Available online at www.sciencedirect.com

SciVerse ScienceDirect

Ceramics International 39 (2013) 1351–1358

CERAMICS INTERNATIONAL

www.elsevier.com/locate/ceramint

The synthesis of the particulates Al matrix composites by the compocasting method

Mohsen Ostad Shabani, Ali Mazahery*

Karaj Branch, Islamic Azad University, Karaj, Iran

Received 4 July 2012; received in revised form 19 July 2012; accepted 22 July 2012
Available online 27 July 2012

Abstract

Many scientific and engineering applications require optimization methods to find more than one solution to multimodal optimization problems. This paper presents an experimental and computational investigation on the influences of the secondary mechanical processing with different reductions on the porosity, microstructure and mechanical properties of compocast high strength and highly uniform Al matrix composites. Multiple solutions to the problems are located and refined using a new particle swarm optimization (PSO) technique. The technique, NichePSO, extends the inherent unimodal nature of the standard PSO approach by growing multiple swarms from an initial particle population. Each subswarm represents a different solution or niche; optimized individually. The outcome of the NichePSO algorithm is a set of particle swarms, each representing a unique solution. The as-cast composite exhibited higher porosity content as compared with the composite in the rolled conditions. Furthermore, the tensile strength of the composites increased considerably by increasing the reduction ratio in the cold rolling process.

Keywords: Synthesis; Metal matrix; Microstructure

1. Introduction

During the last decade, the development in optimization theory saw the emergence of swarm intelligence, a category of random search methods of solving global optimization problems. Ant colony (AC) and particle swarm optimization (PSO) are two paradigms of this kind of methods, and recently have shown to be efficient tools for solving the MSA problem [1–5]. The PSO algorithm was originally proposed by Kennedy as a simulation of social behavior of bird flock. It can be easily implemented and is computationally inexpensive, since its memory and CPU speed requirements are low. PSO has been proved to be an efficient approach for many continuous global optimization problems and in some cases it does not suffer the difficulties encountered by GA [6–9]. During the last decade, there have been a lot of remarkable developments in the field of PSO, particularly in improvements and applications of the algorithm. The concept of PSO is inspired by the flocking behavior of the birds. It was first proposed by Kennedy in 1995. Like evolutionary algorithms PSO is also a population based heuristic, where the population of the potential solutions is called a swarm and each individual solution within the swarm, is called a particle. In order to simulate the behavior of the swarm, each particle is allowed to fly towards the optimum solution [10–15].

During the last decade novel computational methods have been introduced in some fields of engineering sciences, including the solidification and deformation of metal matrix composites in materials science. There are several manufacturing techniques for particle reinforced MMCs such as liquid metal infiltration, spray decomposition, squeeze casting, compocasting, powder metallurgy and mechanical alloying. Stir casting of MMCs is an attractive processing method for these advanced materials since it is relatively inexpensive, and offers a wide variety of material and processing condition options. Generally, these composites consist of a metal matrix, which is melted during casting, and ceramic reinforcement which is added to the molten matrix material by a mechanical stirrer. In this method, incorporation of the reinforcement into the

*Corresponding author. Tel.: +98 912 563 6709; fax: +98 261 6201888.
E-mail address: chorookdyingbride@yahoo.com (A. Mazahery).

0272-8842/$ - see front matter © 2012 Elsevier Ltd and Techna Group S.r.l. All rights reserved.
http://dx.doi.org/10.1016/j.ceramint.2012.07.073

melt and pouring of the composite slurry into the mold are carried out in a fully liquid state (i.e., above liquidus temperature of the matrix alloy). Different researches have shown that introduction and uniform dispersion of reinforcements into the liquid matrices is very difficult due to the poor wetting of ceramic particles by molten alloys [16,17]. In order to overcome some of the drawbacks associated with the conventional stir casting techniques, semisolid agitation processes can be employed. The benefits include reduced solidification shrinkage, lower tendency for hot tearing, suppression of segregation, settling or agglomeration and faster process cycles. These advantages are accompanied with lack of superheat (lower operating temperatures) as well as a lower latent heat which results in a longer die life together with a reduced chemical attack of the reinforcement by alloy, also a globular, non-dendritic structure of the solid phase which then explains the thixotropic behavior of the material [18–20].

A commercial AA6061 aluminum alloy is one of the Al–Mg–Si (Cu) system alloys that can be significantly hardened by a proper heat treatment. Because of its medium strength, excellent corrosion resistance, and weldability, the AA6061 alloy has been widely used as structural material for construction, transportation and sports.

The purpose of this study is firstly to investigate the effects of the secondary mechanical processing on the microstructures and mechanical properties of AA6061 aluminum alloy matrix composites produced by the compocasting. Another objective is to solve the global optimization problems using a category of random search methods which helps to increase the possibility for industry application and also to obtain mass-producible material with improved mechanical properties.

2. Experimental procedure

Al composites reinforced with the B_4C particles have been used for the present study. The AA6061 aluminum alloy was produced from 99.9 wt% pure aluminum which had been melted and then pure silicon, master alloy of Al–75 wt%Cr, Al–50 wt%Cu, and pure magnesium were added in order. The melted alloy was cast into a metal mold with the inner dimensions of 125 mm × 100 mm × 25 mm after degassing for 30 min. The chemical composition of the AA6061 is Al–1.1Mg–0.7Si–0.3Cu–0.2Cr in weight percentage. The wettability of B_4C particles represents a very important issue which is poor at temperatures near the melting point of aluminum (660 °C) [21]. It is reported that that B_4C powders coated with some of Ti-compounds might have reasonable wettability with aluminum [22–26].

In this study, the B_4C powders were coated with TiB_2 via a sol–gel process [25]. The composite was synthesized through a semisolid processing route using coated B_4C particle sizes of 1, 5, 20 and 50 μm as the reinforcement. The process involved melting the alloy in the graphite crucible using an electrical resistance furnace. The furnace is controlled using a J-type thermocouple located inside the gas chamber. The temperature of the alloy was raised to about 680 °C and stirred at 400/500/600/700 rpm using an impeller fabricated from graphite and driven by a variable ac motor. The stirring time were noted at 5, 10 and 15 min after the addition of B_4C during the process.

The temperature of the furnace was gradually lowered until the melt reached a temperature in the liquid solid state (corresponding to 0.2 solid fraction) while stirring was continued. The stirrer was positioned just below the surface of the slurry and the coated particles were added uniformly at a rate of 50 g/min over a time period of approximately 3 min. The casting was obtained by pouring composite slurry into steel die placed below the furnace. A continuous purge of nitrogen gas is used inside and outside of the crucible to minimize the oxidation of molten aluminum. The obtained casts were annealed at 530 °C for 2 h, machined to samples of 150 mm length, 50 mm width and 10 mm thickness and cold rolled to different final reduction.

The experimental density of the composites was obtained by the Archimedes method of weighing composites first in air and then in water, while the theoretical density was calculated using the mixture rule according to the volume fraction of the B_4C particles. Metallographic samples were prepared using standard metallographic techniques, etched with standard aluminum etching solutions and examined by a scanning electron microscope to determine the distribution of the B_4C particles. The volume fraction of B_4C particles was measured by means of an image analyzer system attached to the optical microscope. The distribution of the B_4C particles within the matrix alloy was characterized by a distribution factor (DF) defined as $DF = S.D./A_f$ in which A_f is the mean value of the area fraction of the B_4C particles measured on 100 fields of a sample and S.D. is its standard deviation. A non-uniform microscopic distribution of the reinforcing phase within a sample is reflected as a relatively high value of DF. The tensile test samples were machined according to the ASTM E8M standard [24] and oriented along the rolling direction.

3. Modeling

Different PSO models have been developed based on the neighborhood topology particles use to exchange information about the search space [12]. In the g_{best} model, which is used in this paper, the best particle is determined from the entire swarm and all other particles flock towards this particle [14]. If the position of the best particle is denoted by the vector **y**, for each iteration of a g_{best} PSO, the *j*th-dimension of particle i's velocity vector, V_i, and its position vector, X_i, is updated as follows:

$$V_{i+1}^{t+1} = wV_{ij}^{t} + c_1 r_{1j}(y^{t}_{ij} - X_{ij}^{t}) + c_2 r_{2j}(\rightarrow y^{t}_{ij} - X_{ij}^{t}) \quad (1)$$

$$X_i^{t+1} = V_i^{t+1} + X_i^{t} \quad (2)$$

where c_1 and c_2 are the two positive constants, called cognitive learning rate and social learning rate, respectively; r_1 and r_2 are a random function in the range [0,1]; w is the inertia factor which linearly decreases from 0.9 to 0.2 through the search process. In addition, the velocities of the particles are confined within $[V_{min}, V_{max}]^D$. If an element of velocities exceeds the threshold V_{min} or V_{max}, it is set equal to the corresponding threshold. This section provides a short summary of, where it is shown that the standard g_{best} PSO cannot locate multiple solutions, and that the standard l_{best} PSO is inefficient in doing so. For the g_{best} PSO, Van den Bergh, and Clerc formally proved that all particles converge on a single attractor, which is a weighted average of the global best position and the personal best position of the particle [13]. These formal proofs clearly show that the g_{best} PSO cannot locate, in the same execution of the algorithm, more than one solution. If the g_{best} PSO is executed a number of times, each time from different initial conditions, it may be the case that more than one unique solution is found. However, there is no such guarantee.

In fact, there is not even a guarantee that the solution found is a local optimum, as proven in. The proof of convergence to the weighted average of personal best and global best positions has been done with respect to g_{best} PSO, and cannot be directly applied to l_{best} PSO. Based on this proof, the only thing that can be said is that for each neighborhood, a particle converges to a weighted average of its personal best and neighborhood best solutions. Since neighborhoods are constructed based on particles indices with some overlap between neighborhoods, it is intuitively expected that the neighborhoods, will eventually converge on the same point [10]. However, no such proof exist. Engelbrecht empirically showed that, for the l_{best} PSO, particles do form subgroups, which can be perceived as niches. Even if these subgroups can be considered as niches, it was shown in that only a small number of solutions are found, and only when large swarm sizes are used. The conclusion from is that the standard l_{best} PSO is inefficient in locating multiple solutions. The inability of g_{best} PSO and the inefficiency of l_{best} PSO in locating multiple solutions motivates research in the modification of the standard PSO to promote niching within a single swarm [12–14].

The NichePSO algorithm is a PSO based niching technique [9]. Niches are identified by monitoring changes in the fitness of individual particles in a swarm. The initial swarm is known as the 'main' swarm. When a particle representing a candidate solution is found, a subswarm is created with this particle and its closest neighbor. Subswarms are grown from the 'main' swarm. When all particles from the main swarm have been depleted, no further subswarms can be created. Subswarms that occupy regions in the search space that may represent the same niche are merged. To avoid this problem, any particle that occupies a position that can be considered to fall within an existing swarm is also added to the swarm [10].

3.1. Initialization

The general location of potential solutions in a search space may not always be known in advance. It is therefore a good policy to distribute particles uniformly throughout the search space before learning commences. To ensure a uniform distribution, Faure-sequences are used to generate initial particle positions. Faure-sequences are distributed with high uniformity within a n-dimensional unit cube. Other pseudo-random uniform number generators, such as Sobol-sequences, may also be used [12–14].

3.2. Main swarm training

In the nbest algorithm, overlapping particle neighborhoods discourage convergence on local optima. To this end, NichePSO uses a technique that frees a particle from the influence of a neighborhood or global best term in the velocity update equation [8]. When a particle considers only its own 'history and experiences' in the form of a personal best, it can converge on a local optimum as it is not drawn to a position in the search space that has better fitness as a result of the traversal of other particles. This search approach has been previously investigated [10]. Kennedy and Eberhart [13] referred to it as the cognition only model, in recognition of the fact that only a conscience factor, in the form of the personal best $\mathbf{y}_i$, is used in the update. No social information, such as the global best solution in the g_{best} and l_{best} algorithms, will influence position updates. This arrangement allows each particle to perform a local search.

3.3. Identification of niches

A fundamental question when searching for different niches is how to identify them. The objective function's landscape is then stretched to keep other particles from exploring this area in the search space. If the isolated particle's fitness is not close to a desired level, the solution can be refined by searching the surrounding function landscape with the addition of more particles [8,9].

3.4. Absorption of particles into a subswarm

When a particle is still a member of the main swarm, it has no knowledge of subswarms that may have been created during the execution of the NichePSO learning algorithm. It is therefore quite likely that a particle may venture into an area of the search space that is being independently optimized by a subswarm [10]. Such particles are merged with the corresponding subswarm, based on the following suppositions:

- Including a particle traversing the search space of an existing subswarm, may expand the diversity of the subswarm, thereby more rapidly leading to solutions with better fitness.

- An individual particle moving towards a solution on which a subswarm is working, will make much slower progress than what would have been the case had social information been available to ensure that position updates move towards the particle's known favorable solution.

3.5. Merging subswarms

A subswarm is created by removing a particle that represents an acceptable candidate solution from the main swarm, as well as a particle that lies closest to it in the search space, and to group these into a subswarm. From this rule, it follows that particles in subswarms all represent similar solutions. This can lead to subswarms with radii that are very small, and even radii approximating zero. Consequently, when a particle approaches a potential solution it may not necessarily be absorbed into a subswarm already optimizing the particular solution. If the particle has an acceptable fitness, another subswarm will be created at its position in the search space. If two solutions are very similar, a single subswarm will be created to optimize both solutions [8]. Eventually, only one of these solutions will be maintained. This introduces a dilemma, as multiple swarms will attempt to optimize the same solution. To alleviate this situation, subswarms may be merged when the hyper-space defined by their particle positions and radii intersect in the search space.

3.6. Stopping criteria

When each individual subswarm has located a solution and stably maintained it for a number of training iterations, the NichePSO may be considered to have converged. Each swarm must converge on a unique solution. Typically, a subswarm is considered to have converged when its global best solution's fitness is either above or below a threshold value, depending on whether the fitness function describes a maximization or minimization problem. Fitness threshold criteria can not, however, detect acceptable solutions in a multi-modal fitness function where local and global maxima exist. Local maxima are never considered to be acceptable solutions, as their fitness do not necessarily adhere to possibly strict threshold values [8–10]. Any algorithm that therefore depends solely on threshold values will fail to converge. Therefore, the change in particle positions are tracked over a number of iterations. If no significant change occurs in their positions, such as may be detected by considering their variance over a small number of training iterations, the subswarm may be considered to have converged. The algorithm may also be stopped after a maximum number of training iterations.

4. Experimental results

The microstructures of the coated composites were examined by SEM microscope in order to determine the distribution of the B_4C particles and presence of porosity. Typical SEM micrographs of the compocast B_4C reinforced Al alloy composites are shown in Fig. 1. It is observed that the fabrication of these composites via the compocasting technique plus reduction (90%) during cold rolling process leads to reasonably uniform distribution of particles in the matrix and minimum clustering or agglomeration of the reinforcing phase.

Fig. 2 shows the effect of the rolling process on the porosity content of the composites. It is noted that the application of the heavy reduction (90%) during cold rolling process results in approximately 0% volume fraction porosity. Porosity formation in cast metal matrix composites can be attributed to the air trapped in the clusters of particles as well as the hindered metal flow inside them. It also indicates that increasing amount of porosity is observed with increasing the volume fraction of B_4C particulates. The porosity level increased, since the contact surface area was increased. This is attributed to pore nucleation at the B_4C particulate sites (porosity associated with individual particle) and to hindered liquid

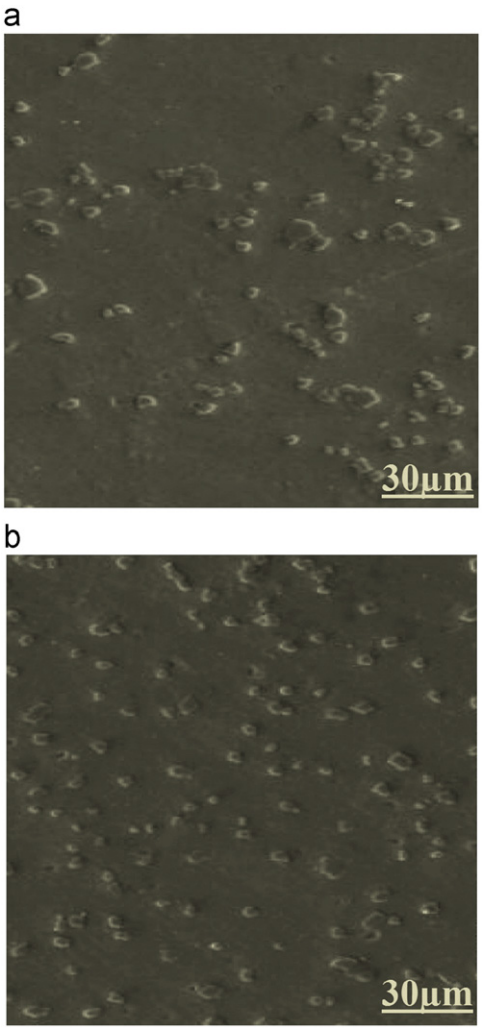

Fig. 1. SEM micrographs of the Al matrix composites reinforced with 15% B_4C: (a) the as-cast composites and (b) cold rolled composites (90%).

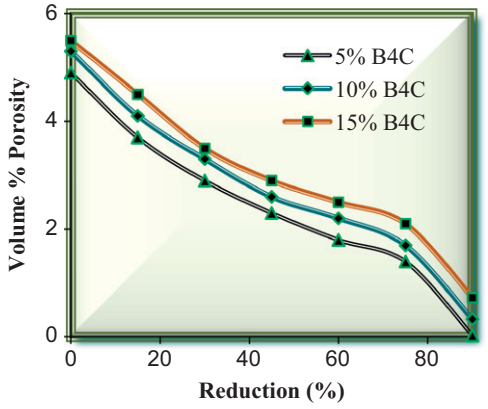

Fig. 2. The effect of the rolling process and B_4C volume fraction on the porosity content of the composites.

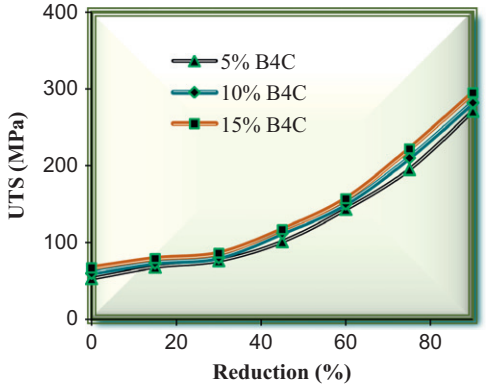

Fig. 3. The effect of the rolling process and B_4C volume fraction on the tensile strength of the composites.

metal flow due to more particle clustering (porosity associated with the particle clusters) [12,27].

The decreased porosity of MMCs during rolling is due to the flow of the matrix alloy under the applied shear and compressive forces resulting in filling the voids. The increased rolling reduction provides easier flow of the matrix alloy and hence results in decreased porosity. In fact, the major reason for rolling the particulate metal matrix composites (PMMCs) is to close the pores and attain improved mechanical properties.

The strength results of the composites are shown in Fig. 3. It is noted that there would be a great enhancement in tensile behavior of the composites while using rolling reduction in comparison to the as-cast composites. It can also be seen that tensile strength increases when the reduction quantity is increased. The uniformity in distribution of particles within the sample is a microstructural feature which determines the in-service properties of particulate AMCs. A non-homogeneous particle distribution in cast composites arises as a consequence of sedimentation (or flotation), agglomeration and segregation. The subject of particle distribution in particulate MMCs has been studied by several investigators either qualitatively or quantitatively. The macroscopic particle segregation due to gravity (settling) has also been studied both experimentally and theoretically, the latter of which generally involves the correlation of particle settling rate within the composite slurry with the Stocks' law [28–32]. A sedimentation experiment was conducted on the composites containing 10 vol% particles. Fig. 4 shows the B_4C concentration as a function of the distance from the bottom of the mold (D). It is noted that the particle distribution in the cold rolled composites is much more uniform than the as-cast one. As can be seen, the lower parts of the as-cast ingot contained a lower volume percent of particles than the upper parts, representing an uneven macroscopic particle distribution.

During the solidification process of the composite slurries, the reinforcing particles are pushed to the interdendritic or intercellular regions and tend to segregate along the grain boundaries of matrix alloy. The quantitative assessment of the B_4C particle distribution within composite samples was performed by considering the distribution factor (DF) defined as:

$$DF = S.D./A_f \quad (3)$$

In which A_f is the mean value of the area fraction of the B_4C and S.D. is its standard deviation. Fig. 5 shows the gradual decrease in DF for the composites when the particle content and cold rolling reduction increased, indicating the improvement in the uniformity of the B_4C particle distribution. These results can be attributed the occurrence of deagglomeration process in the cold rolled composites. Deagglomeration phenomenon is the result of high deformation ratio applied to the aluminum matrix. Plastic flow of the aluminum matrix causes the B_4C clusters to break and get separated from each other, resulting in a more uniform distribution of the particles in the matrix. This improvement in the tensile strength of the deformed samples also indicates that the use of cold rolling helps to disperse B_4C particulates more uniformly through the Al matrix which leads to higher dislocation density and plastic constraint in the matrix of the composite.

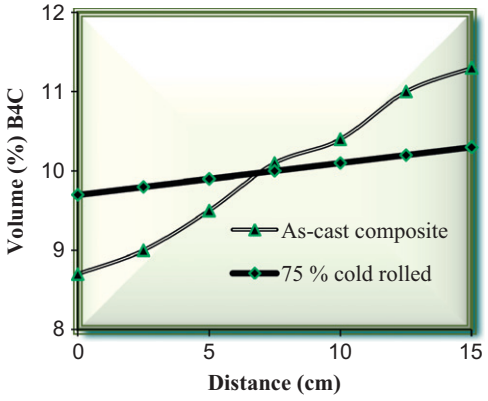

Fig. 4. The B_4C concentration as a function of the distance from the bottom of the mold (D).

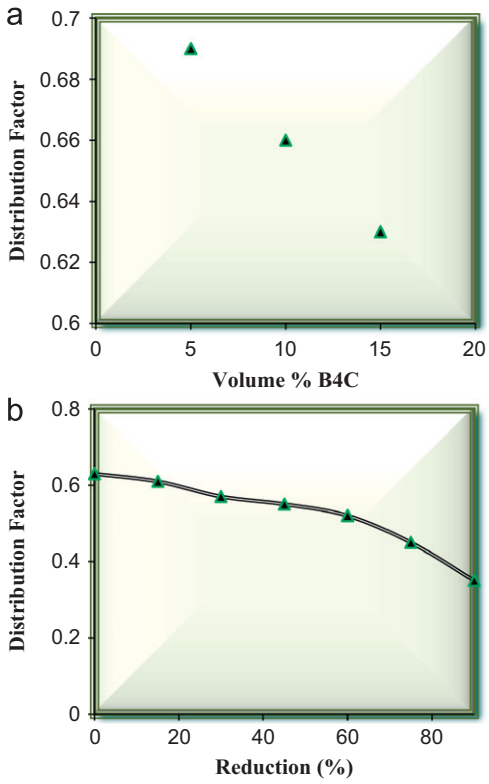

Fig. 5. Distribution factor versus: (a) volume fraction of B_4C and (b) reduction (%).

The strain-hardening of composites is expected to be influenced by the dislocation density, dislocation-to-dislocation interaction and constraint of plastic flow due to resistance offered by particles. It is observed that the flow stress of the composite enhances with increase in reduction ratio. The matrix could flow only with the movement of B_4C particles or over the particles during plastic deformation. While distribution is more uniform, the matrix gets constraint considerably to the plastic deformation because of smaller inter-particle distance and thus results in higher degree of improvement in flow stress and UTS. Normally micron-sized particles are used to improve the ultimate tensile and the yield strengths of the metal. However, the ductility of the MMCs deteriorates significantly with high ceramic particle concentration. Fig. 6 shows the elongation results of the as-cast and cold rolled composites. It is observed that there is a simultaneous improvement in the strength and ductility of the cold rolled composites which might be explained by the reduction in porosity content.

5. Modeling results

For each of the three test functions, 35 experiments were done with the NichePSO algorithm with $c_1=c_2=1.1$. The inertia weight w was scaled linearly from 0.9 to 0.2 over a maximum of 6000 iterations of the algorithm. A mean absolute percentage error (MAPE) is used to evaluate the

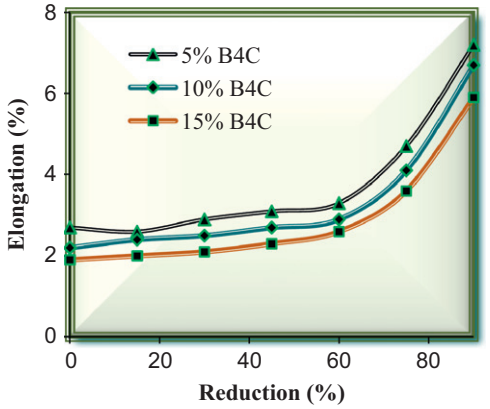

Fig. 6. The effect of the rolling process and B_4C volume fraction on the elongation of the composites.

forecasting accuracy, which is as follows:

$$MAPE = \left[\frac{1}{Q}\sum_{Q=1}^{Q}\left|\frac{A-F}{A}\right|\right]100 \quad (4)$$

where A and F represent the actual and forecasting values respectively and Q is the number of forecasting points. Fig. 7 shows the effect of iteration number on the MAPE of developed model. These parameters were chosen to ensure convergent trajectories. NichePSO successfully located all global maxima of all the functions tested [8]. Unimodal optimization techniques, such as the standard PSO and GAs, fail to efficiently locate multiple solutions to multi-modal problems because of their inherent unimodal optimization nature [33–39]. These algorithms need to be extended to facilitate niching and speciation abstractions. NichePSO is no exception—although the essence of the original PSO is retained, a number of extensions were made. The motivations and reasoning behind these extensions are presented, justified and investigated in this section. The following issues are considered:

- the relationship between the initial swarm size and the number of solutions in a multi-modal fitness function, and
- scalability of the algorithm on highly multi-modal functions.

Each subswarm created by the NichePSO algorithm can be seen as a hyper-sphere in a search space [9]. The hyper-sphere's radius is determined by the Euclidean distance between the swarm's global best position and the particle in the swarm that lies furthest from it. Two subswarms are merged when the two conceptual hyper-spheres represented by them overlap. When all particles in a swarm have converged on a single solution, a swarm will have an effective radius of zero. Final optimized parameters are 690 s stirring time, 620 rpm speed of stirrer, 31.43 μm particle size of B_4C, 6.53% volume percentage of B_4C, 90% reduction, 0.43% porosity, 277.21 MPa UTS and

Fig. 7. The effect of iteration number on the MAPE.

6.73% elongation. The results show that the novel technique implemented in this investigation has an acceptable performance. Therefore, this work shows the usefulness of an intelligent way to predict the performance of Al matrix composites using NichePSO.

6. Conclusion

Population-based search methods such as particle swarm optimizers, present a real and viable alternative to existing numerical optimization techniques. Population based optimization techniques can rapidly search large and convoluted search spaces and are not susceptible to suboptimal solutions. The standard g_{best} and l_{best} PSO approaches share information about a best solution found by the swarm or a neighborhood of particles. Sharing this information introduces a bias in the swarm's search, forcing it to converge on a single solution. Experimental investigations of the composites after 90% reduction showed an excellent uniform distribution of boron carbide particles in the matrix. In fact, the major reason for rolling the particulate metal matrix composites is to close the pores and attain improved mechanical properties. During cold rolling process it was observed that the tensile strength and ductility of the samples increased by increasing the reduction content.

References

[1] Q. Lu, P. Luo, A learning particle swarm optimization algorithm for odor source localization, International Journal of Automation and Computing 8 (3) (2011) 371–380.
[2] M.O. Shabani, A. Mazahery, The ANN application in FEM modeling of mechanical properties of Al–Si alloy, Applied Mathematical Modelling 35 (2011) 5707–5713.
[3] E. Gomes, M.H. Rahul, Particle swarm optimization approaches for constrained engineering design problems, International Journal of Expert Systems 22 (2010) 155–163.
[4] L. dos Santos Coelho, P. Alotto, Global optimization of electromagnetic devices using an exponential quantum-behaved particle swarm optimizer, IEEE Transactions on Magnetics 44 (2008) 1074–1077.
[5] A. Mazahery, M.O. Shabani, A356 reinforced with nanoparticles: numerical analysis of mechanical properties, Journal of the Minerals Metals and Materials Society 64 (2012) 323–329.
[6] R.A. Krohling, E. Mendel, Bare bones particle swarm optimization with Gaussian or Cauchy jumps, in: IEEE Congress on Evolutionary Computation, 2009, CEC'09, pp. 3285–3291.
[7] M.O. Shabani, A. Mazahery, M.R. Rahimipour, A.A. Tofigh, M. Razavi, The most accurate ANN learning algorithm for FEM prediction of mechanical performance of alloy A356, Kovove Materialy-Metallic Materials 50 (2012) 25–31.
[8] D. Beasley, D.R. Bull, R.R. Martin, A sequential niching technique for multimodal function optimization, Evolutionary Computation 1 (2) (1993) 101–125.
[9] R. Brits, Niching Strategies for Particle Swarm Optimization. Master's Thesis, Department of Computer Science, University of Pretoria, Pretoria, South Africa, November 2002.
[10] A.P. Engelbrecht, B.S. Masiye, G. Pampara, Niching ability of basic particle swarm optimization algorithms, in: Proceedings of the IEEE Swarm Intelligence Symposium, 2005.
[11] M.O. Shabani, A. Mazahery, Artificial intelligence in numerical modeling of nano sized ceramic particulates reinforced metal matrix composites, Applied Mathematical Modelling 36 (2012) 5455–5465.
[12] J. Kennedy, R.C. Eberhart, Particle swarm optimization, in: Proceedings of the IEEE International Conference on Neural Networks, vol. IV, Perth, Australia, 1995, pp. 1942–1948.
[13] J. Kennedy, R.C. Eberhart, Swarm Intelligence, Morgan Kaufman, 2001.
[14] J. Kennedy, R. Mendes, Population structure and particle swarm performance, in: Proceedings of the IEEE World Congress on Evolutionary Computation, Honolulu, Hawaii, May 2002, pp. 1671–1676.
[15] F. van den Bergh, A.P. Engelbrecht, A study of particle swarm optimization particle trajectories, Information Science 176 (8) (2006) 937–971.
[16] A. Mazahery, M.O. Shabani, Study on microstructure and abrasive wear behavior of sintered Al matrix composites, Ceramics International 38 (5) (2012) 4263–4269.
[17] M.O. Shabani, A. Mazahery, The performance of various artificial neurons interconnections in the modelling and experimental manufacturing of the composites, Materiali in Tehnologije 46 (2) (2012) 109–113.
[18] C.J. Quaak, W.H. Kool, Properties of semisolid aluminium matrix composites, Materials Science and Engineering A 188 (1994) 277–282.
[19] J. Hashim, L. Looney, M.S.J. Hashmi, Particle distribution in cast metal matrix composites. Part I, Journal of Materials Processing Technology 123 (2002) 251–257.
[20] A. Mazahery, M.O. Shabani, Tribological behavior of semisolid–semisolid compocast Al–Si matrix composites reinforced with TiB_2 coated B_4C particulates, Ceramics International 38 (2012) 1887–1895.
[21] W.R. Blumenthal, G.T. Gray, T.N. Claytor, Response of aluminium-infiltrated boron carbide cermets to shock wave loading, Journal of Materials Science 29 (1994) 4567.
[22] A.J. Pyzik, I.A. Aksay, M. Sarikaya, Processing and microstructural characterization of B_4C–Al cermets, Materials Science Research 21 (1986) 45.
[23] A.J. Pyzik, I.A. Aksay, Processing of ceramic and metal matrix composites, in: Proceedings of the International Symposium on Advances in Processing of Ceramic and Metal Matrix Composites, New York, 1989, pp. 269.
[24] M.O. Shabani, A. Mazahery, Application of FEM and ANN in characterization of Al matrix nano composites using various training algorithms, Metallurgical and Materials Transactions A 43 (2012) 2158–2165.
[25] A.J. Pyzik, D.R. Beaman, Al–B–C phase development and effects on mechanical properties of B_4C/Al-derived composites, Journal of the American Ceramic Society 78 (1995) 305.
[26] S.K. Rhee, Wetting of AlN and TiC by liquid Ag and liquid Cu, Journal of the American Ceramic Society 53 (1970) 386.
[27] A. Mazahery, M.O. Shabani, M.R. Rahimipour, A.A. Tofigh, M. Razavi, Effect of coated B_4C reinforcement on mechanical properties of squeeze cast A356 composites, Kovove Materialy-Metallic Materials 50 (2012) 107–113.

[28] L.V. Vugt, L. Froyen, Gravity and temperature effects on particle distribution in Al–Si/SiCp composites, Journal of Materials Processing Technology 104 (2000) 133–144.
[29] G.A. Irons, K. Owusu-Boahen, Settling and clustering of silicon carbide particles in aluminium metal matrix composites, Metallurgical and Materials Transactions B 26 (1995) 980–981.
[30] M.O. Shabani, A. Mazahery, The GA optimization performance in the microstructure and mechanical properties of MMNCs, Transactions of the Indian Institute of Metals 65 (1) (2012) 77–83.
[31] M. Gupta, L. Lu, S.E. Ang, Effect of microstructural features on the aging behavior of Al–Cu/SiC metal matrix composites processed using casting and rheocasting routes, Journal of Materials Science 32 (1997) 1261–1267.
[32] P.A. Karnezis, G. Durrant, B. Cantor, Characterization of reinforcement distribution in cast Al-alloy/SiC composites, Materials Characterization 40 (1998) 97–109.
[33] A. Mazahery, M.O. Shabani, Process conditions optimization in Al–Cu alloy matrix composites, Powder Technology 225 (2012) 101–106.
[34] D. Parrott, X. Li, Locating and tracking multiple dynamic optima by a particle swarm model using speciation, IEEE Transactions on Evolutionary Computation 10 (4) (2006) 440–457.
[35] C.H. Wu, N. Dong, W.H. Ip, C.Y. Chen, K.L. Yung, Z.Q. Chen, Chaotic hybrid algorithm and its application in circle detection, Lecture Notes in Computer Science 6024 (2010) 302–311.
[36] M.O. Shabani, A. Mazahery, Microstructural prediction of cast A356 alloy as a function of cooling rate, Journal of the Minerals Metals and Materials Society (2012) 132–136.
[37] S.Z. Zhao, P.N. Suganthan, Two-l_{bests} based multi-objective particle swarm optimizer, Engineering Optimization 43 (1) (2011) 1–17.
[38] P. Sathiya, S. Aravindan, A.N. Haq, K. Paneerselvam, Optimization of friction welding parameters using evolutionary computational techniques, Journal of Materials Processing Technology 209 (2009) 2576–2584.
[39] M.O. Shabani, A. Mazahery, Optimization of process conditions in casting aluminum matrix composites via interconnection of artificial neurons and progressive solutions, Ceramics International 38 (2012) 4541–4547.